Analysis of the Various Elements of Heat Sources in Silicon Carbide Polymers (6H-SiC and 3C-SiC) Semiconductor Laser

SAEID MARJANI[1,*], RAHIM FAEZ[2] and HAMID MARJANI[3]

[1]Young Researchers Club, Arak Branch, Islamic Azad University, Arak, Iran
[2]Department of Electrical Engineering, Sharif University of Technology, Tehran, Iran
[3]Department of Electrical Engineering, Arak Branch, Islamic Azad University, Arak, Iran

*Corresponding author: E-mail: saeidmarjani@yahoo.com

In the present paper, we investigated the various elements of heat sources within a silicon carbide polymers (6H-SiC and 3C-SiC) semiconductor laser. The device employs 3C-SiC quantum well (QW) which is sandwiched between two layers of 6H-SiC as cladding regions that can be interpreted in terms of a type-II heterostructure character and a built-in electric field due to the pyroelectricity of 6H using a numerical simulator. The basic design goal was the study of the various elements of heat sources, including the Joule heat power, the Peltier-Thomson heat power and the recombination heat power.

Key Words: Modeling, Heat sources, Silicon carbide polymers, Semiconductor laser.

INTRODUCTION

During the past decades, silicon carbide (SiC) has been praised as a promising semiconductor material for high power, high-frequency and high-temperature electronics and optoelectronic devices, where the existing Si or GaAs technology cannot provide any satisfactory performance. This intensive research effort resulted in the commercialization of the first SiC-based devices in year 2001 namely, high power Schottky diodes[1]. Properties such as the large breakdown electric field strength, large saturated electron drift velocity, small dielectric constant, reasonably high electron mobility and high thermal conductivity make silicon carbide an attractive candidate for fabricating power devices with reduced power losses and die size[2].

Silicon carbide has many stable polytypes, including cubic zinc-blende, hexagonal and rhombohedral polytypes. In the cubic zinc-blende structure, labeled as 3C-SiC or β-SiC, Si and C occupy ordered sites in a diamond framework. In hexagonal polytypes nH-SiC and rhombohedral polytypes n R-SiC, generally referred to as αη-SiC, *n*-Si-C bilayers consisting of C and Si layers stack in the primitive unit cell. The lattice structures of the 3C-SiC and 6H-SiC phases are presented in Fig. 1[3].

Lattice heat is generated whenever physical processes transfer energy to the crystal lattice. According to differences in transfer mechanisms, heat sources can be separated into Joule heat, electron-hole recombination heat, Thomson heat
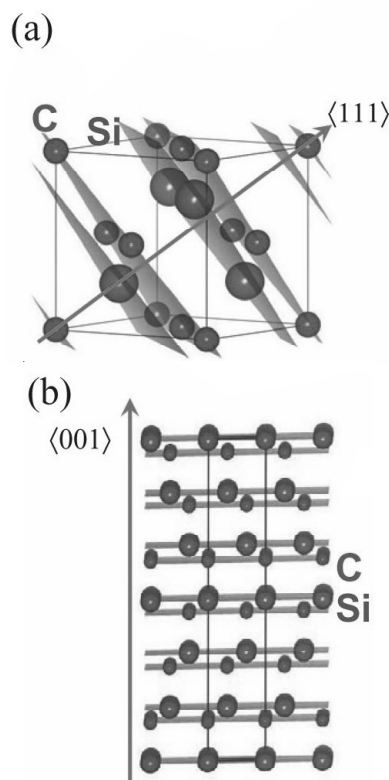
Fig. 1.   (a) Unit cell of cubic 3C-SiC. (b) Four unit cells of hexagonal 6H-SiC

and heat from optical absorption. Self-heating often limits the performance of optoelectronic devices. Heat is generated when carriers transfer part of their energy to the crystal lattice. In consequence, the thermal energy of the lattice rises, which is measured as an increase in its temperature[4].

In this paper, we studied the various elements of heat sources within a silicon carbide polymers (6H-SiC and 3C-SiC) semiconductor laser.

In the following, we first briefly describe the numerical model and the structure of edge emitting laser. Next we present the obtained numerical results. Finally, the conclusions provide common guidelines for designing performance of edge emitting laser.

THEORY AND MODEL

In modeling edge emitting laser, we must consider the electrical, optical and thermal interaction during laser performance. Thus base of simulation is to solve Poisson and continuity equations for electrons and holes[5]. Poisson's equation is defined by:

$$\nabla(\varepsilon\nabla\psi) = \rho \tag{1}$$

where ψ is electrostatic potential, ρ is local charge density and ε is local permittivity. The continuity equations of electron and hole are given by Piprek[4]:

$$\frac{dn}{dt} = G_n - R_n + \frac{1}{q}\nabla j_n \tag{2}$$

$$\frac{dp}{dt} = G_p - R_p + \frac{1}{q}\nabla j_p \tag{3}$$

where n and p are the electron and hole concentration, J_n and J_p are the electron and hole current densities, G_n and G_p are the generation rates for electrons and holes, R_n and R_p are the recombination rates and q is the magnitude of electron charge.

The fundamental semiconductor eqns. 1-3 are solved self-consistently together with Helmholtz and the photon rate equations. The applied technique for solution of Helmholtz equation is based on improved effective index model[6] which shows accuracy for great portion of preliminary problems. This model is very good adapted to simulation of laser structures and it is often called effective frequency method[7].

Two-dimensional Helmholtz equation is solved to determine the transverse optical field profile and it is given by Silvaco International[5]:

$$\nabla^2 E(r, z, \varphi) + \frac{\omega_0}{c^2}\varepsilon(r, z, \varphi, \omega)E(r, z, \varphi) = 0 \tag{4}$$

where ω is the frequency, $\varepsilon(r, z, f, \omega)$ is the complex dielectric permittivity, $E(r, z, \varphi)$ is the optical electric field and c is the speed of light in vacuum. The light power equation relates electrical and optical models. The photon rate equation is given by Silvaco International[5]:

$$\frac{dS_m}{dt} = \left(\frac{c}{N_{eff}}G_m - \frac{1}{\tau_{ph_m}} - \frac{cL}{N_{eff}}\right)S_m + R_{sp_m} \tag{5}$$

where S_m is the photon number, G_m is the modal gain, R_{spm} is the modal spontaneous emission rate, L represents the losses in the laser, N_{eff} is the group effective refractive index, τ_{phm} is the modal photon lifetime and c is the speed of light in vacuum. The heat flow equation has the form[5]:

$$C\frac{\partial T_L}{\partial t} = \nabla(\kappa\Delta T_L) + H \tag{6}$$

where C is the heat capacitance per unit volume, κ is the thermal conductivity, H is the generation, T_L is the local lattice temperature and H is the heat generation term.

The heat generation equation has the form[5]:

$$H = \left[\frac{\overline{|J_n|^2}}{q\mu_n n} + \frac{\overline{|J_p|^2}}{q\mu_p p}\right] + q(R - G)[\phi_p - \phi_n + T_L(P_p - P_n)]$$

$$- T_L(\overline{J}_n\nabla P_n + \overline{J}_p\nabla P_p) \tag{7}$$

where: $\left[\dfrac{\overline{|J_n|^2}}{q\mu_n n} + \dfrac{\overline{|J_p|^2}}{q\mu_p p}\right]$ is the Joule heating term,

$q(R - G)[\phi_p - \phi_n + T_L(P_p - P_n)]$ is the recombination and generation heating and cooling term, $-T_L(\overline{J}_n\nabla P_n + \overline{J}_p\nabla P_p)$ accounts for the Peltier and Joule-Thomson effects.

Eqns. 1-7 provide an approach that can account for the mutual dependence of electrical, thermal, optical and elements of heat sources. In this paper, we employ numerical-based simulation software to assist in the device design and optimization[5].

Fig. 2 shows the schematic design of 0.83 μm strained quantum-well (QW) laser diode device. In this structure, the active region consists of two 95 nm thick 6H-SiC barrier and 10 nm thick 3C-SiC quantum well (QW). The active region is embedded in 6H-SiC cladding layers with 1500 nm thick.
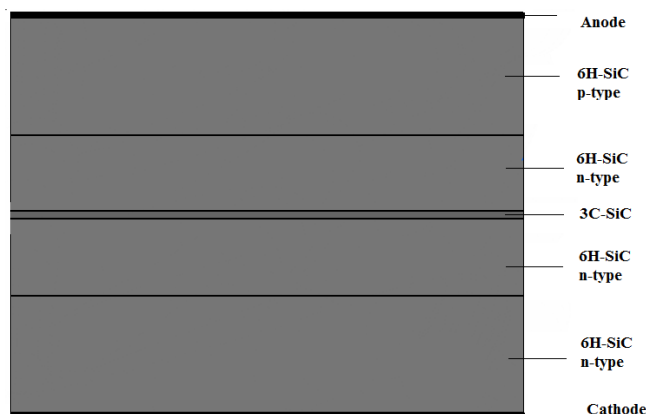
Fig. 2. Schematic structure of the laser device

RESULTS AND DISCUSSION

In this paper, we have used the 6H-SiC/3C-SiC/6H-SiC edge emitting laser and have investigated the various elements of heat sources within the device. Fundamentally, the heat power peaks at the QW region for all heat source elements. The highest contributor of heat power comes from the recombination heat power followed by the Peltier-Thomson heat power and finally the joule heat power. The maximum heat power of the joule, Peltier-Thomson and recombination are 1.3006e7, 5.4123e9 and 5.9835e9 W/cm³, respectively at a bias voltage of 2.5 V.

Fig. 3 shows the joule heat power within a vertical cross-section of the device at a bias voltage of 2.5 V. As can be seen from Fig. 3, get away the quantum well causes the reduction of the joule heat power which should be mainly due to lower current density.
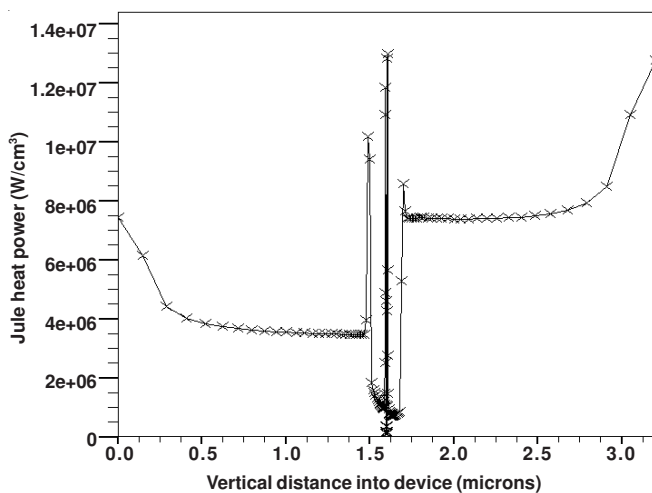
Fig. 3. Joule heat power within the device

Fig. 4 shows the Peltier-Thomson heat power within a vertical cross-section of the device at a bias voltage of 2.5 V. As shown in the Fig. 4, when get away from the quantum well, the Peltier-Thomson heat power shows the same rule as that at the joule heat power which should be mainly due to lower current density. Peltier-Thomson heat is transferred between carriers and lattice as current flows along a gradient of the thermoelectrical power and it changes with the density of states, carrier concentration and temperature. When electrons enter a material with under conduction band edge, they suddenly display extra kinetic energy (hot electrons) that is finally scattered to the lattice *vice-versa* electrons need to receive additional energy from the lattice to leave the quantum well. For that reason, Peltier-Thomson heat can be positive or negative.
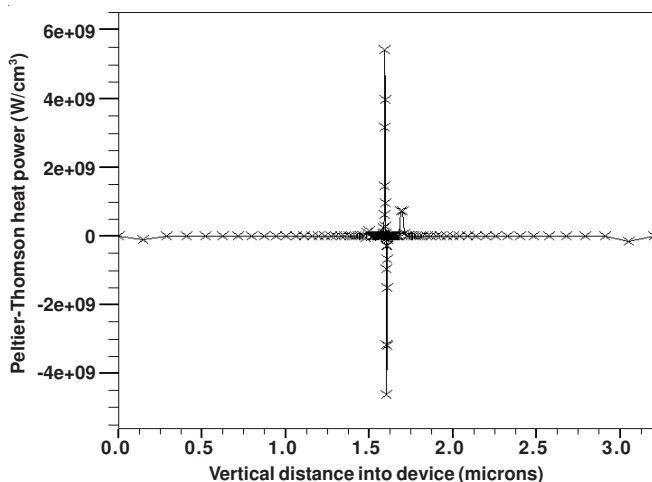
Fig. 4. Peltier-Thomson heat power within the device

Fig. 5 shows the recombination heat power within a vertical cross-section of the device at a bias voltage of 2.5 V. It can be found that, get away from the quantum well, leads to the lower recombination heat power, which should be mainly due to lower net recombination rate, including thermal generation of carriers.
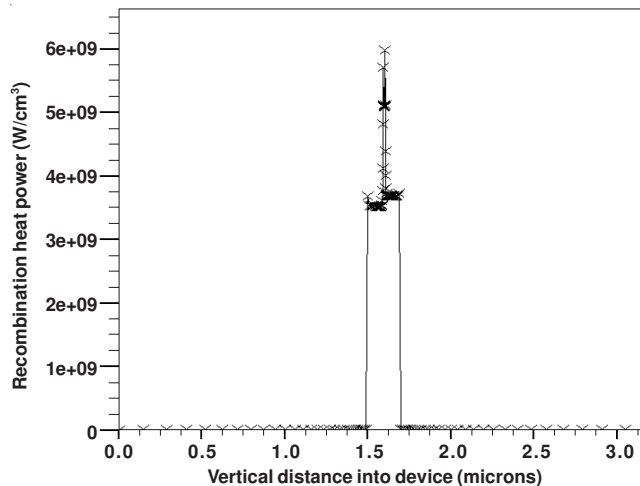
Fig. 5. Recombination heat power within the device

Conclusion

In this paper, we have used the silicon carbide polymers (6H-SiC and 3C-SiC) semiconductor Laser and have evaluated the various elements of heat sources within the device. The results indicate that the highest contributor of heat power comes from the recombination heat power followed by the Peltier-Thomson heat power and finally the joule heat power. The maximum heat power of the joule, Peltier-Thomson and recombination are 1.3006e7, 5.4123e9 and 5.9835e9 W/cm^3, respectively at a bias voltage of 2.5 V.

REFERENCES

1. P.G. Neudeck, In eds.: K.H.J. Bushchow, R.W. Cahn, M.C. Flemings, B. Ilschner, E.J. Kramer and S. Mahajan, Encyclopedia of Materials: Science and Technology (Elsevier Science), Vol. 9, p. 8508 (2001).
2. M. Bhatnagar and B.J. Baliga, IEEE Transactions On Electron Devices, p. 40 (1993).
3. T. Muranaka, Y. Kikuchi, T. Yoshizawa, N. Shirakawa and J. Akimitsu, *Sci. Technol. Adv. Mater.*, 9, 044204 (2008).
4. J. Piprek, Semiconductor Optoelectronic Devices: Introduction to Physics and Simulation, Carrier Transport and Chap. 6 Heat Generation and Dissipation UCSB: Academic Press, Ch. 3, pp. 49-50 and 141-147 (2003).
5. Silvaco International, ATLAS User's Manual, USA, SILVACO International Incorporated (2010).
6. G.R. Hadley, *J. Opt. Lett.*, **20**, 1483 (1995).
7. H. Wenzel and H.J. Wunsche, *IEEE J. Quantum Electronics*, **33**, 1156 (1997).